Spatiotemporal Dynamics of β-Adrenergic cAMP Signals and L-Type Ca^{2+} Channel Regulation in Adult Rat Ventricular Myocytes

Role of Phosphodiesterases

Jérôme Leroy, Aniella Abi-Gerges, Viacheslav O. Nikolaev, Wito Richter, Patrick Lechêne, Jean-Luc Mazet, Marco Conti, Rodolphe Fischmeister, Grégoire Vandecasteele

Abstract—Steady-state activation of cardiac β-adrenergic receptors leads to an intracellular compartmentation of cAMP resulting from localized cyclic nucleotide phosphodiesterase (PDE) activity. To evaluate the time course of the cAMP changes in the different compartments, brief (15 seconds) pulses of isoprenaline (100 nmol/L) were applied to adult rat ventricular myocytes (ARVMs) while monitoring cAMP changes beneath the membrane using engineered cyclic nucleotide-gated channels and within the cytosol with the fluorescence resonance energy transfer–based sensor, Epac2-camps. cAMP kinetics in the two compartments were compared to the time course of the L-type Ca^{2+} channel current ($I_{Ca,L}$) amplitude. The onset and recovery of cAMP transients were, respectively, 30% and 50% faster at the plasma membrane than in the cytosol, in agreement with a rapid production and degradation of the second messenger at the plasma membrane and a restricted diffusion of cAMP to the cytosol. $I_{Ca,L}$ amplitude increased twice slower than cAMP at the membrane, and the current remained elevated for ≈5 minutes after cAMP had already returned to basal level, indicating that cAMP changes are not rate-limiting in channel phosphorylation/dephosphorylation. Inhibition of PDE4 (with 10 μmol/L Ro 20-1724) increased the amplitude and dramatically slowed down the onset and recovery of cAMP signals, whereas PDE3 blockade (with 1 μmol/L cilostamide) had a minor effect only on subsarcolemmal cAMP. However, when both PDE3 and PDE4 were inhibited, or when all PDEs were blocked using 3-isobutyl-l-methylxanthine (300 μmol/L), cAMP signals and $I_{Ca,L}$ declined with a time constant >10 minutes. cAMP-dependent protein kinase inhibition with protein kinase inhibitor produced a similar effect as a partial inhibition of PDE4 on the cytosolic cAMP transient. Consistently, cAMP-PDE assay on ARVMs briefly (15 seconds) exposed to isoprenaline showed a pronounced (up to ≈50%) dose-dependent increase in total PDE activity, which was mainly attributable to activation of PDE4. These results reveal temporally distinct β-adrenergic receptor cAMP compartments in ARVMs and shed new light on the intricate roles of PDE3 and PDE4. **(*Circ Res*. 2008;102:1091-1100.)**

Key Words: cAMP ■ L-type calcium current ■ 5′-3′ cyclic nucleotide phosphodiesterases ■ β-adrenergic receptors ■ compartmentation

cAMP is an ubiquitous second messenger regulating a myriad of cellular functions. In the heart, cAMP mediates the positive inotropic and lusitropic effects of β-adrenergic receptor (β-AR) stimulation by activating the cAMP-dependent protein kinase (PKA), thereby promoting the phosphorylation and activation of key components of the excitation–contraction coupling process. These include the sarcolemmal L-type Ca^{2+} channels ($Ca_V1.2$), which are responsible for the initial Ca^{2+} influx; the ryanodine receptors, which allow Ca^{2+} release from the sarcoplasmic reticulum (SR); troponin I, which controls myofilament sensitivity to Ca^{2+}; and phospholamban, which regulates Ca^{2+} withdrawal from the cytosol and reuptake into the SR.[1]

These phosphorylation events are thought to be tightly regulated by multiprotein signaling complexes organized around A kinase anchoring proteins, thus providing a molecular basis for subcellular compartmentation of the cAMP pathway.[2,3] In support of this view, PKA-mediated phosphorylation gradients were recently reported.[4] However, differential regulation of localized PKA also requires a nonuniform distribution of the PKA activator, cAMP. Indeed, the presence of subcellular compartments with different cAMP con-

Original received November 13, 2007; revision received March 6, 2008; accepted March 13, 2008.

From INSERM U769 (J.L., A.A.-G., P.L., J.-L.M., R.F., G.V.), Châtenay-Malabry, France; Univ Paris-Sud 11 (J.L., A.A.-G., P.L., J.-L.M., R.F., G.V.), Faculté de Pharmacie, Châtenay-Malabry, France; Rudolf-Virchow-Center (V.O.N.), Deutsche Forschungsgemeinschaft-Research Center for Experimental Biomedicine, University of Würzburg, Germany; and Division of Reproductive Biology (W.R., M.C.), Department of Obstetrics and Gynecology, Stanford University School of Medicine, Palo Alto, Calif.

Correspondence to Dr Rodolphe Fischmeister, INSERM U-769, Université Paris-Sud 11, Faculté de Pharmacie, 5, Rue J.-B. Clément, F-92296 Châtenay-Malabry Cedex, France. E-mail fisch@vjf.inserm.fr

Circulation Research **is available at http://circres.ahajournals.org** **DOI: 10.1161/CIRCRESAHA.107.167817**

centrations, also called cAMP microdomains, are inferred from L-type Ca^{2+} channel current ($I_{Ca,L}$) measurements in response to local β-AR stimulation in cardiomyocytes[5] and by direct monitoring of cAMP using fluorescence resonance energy transfer (FRET)-based sensors[6,7] or cyclic nucleotide-gated (CNG) channels.[8] These and other studies[9,10] also underlined the importance of cAMP phosphodiesterases (PDEs) for the spatiotemporal control of cAMP signals.[11]

In the present study, we used a unique approach, combining live-cell imaging and electrophysiology to investigate the spatiotemporal dynamics of β-AR responses in adult rat ventricular myocytes (ARVMs). We performed direct measurements of the cyclic nucleotide level in the subsarcolemmal and cytosolic compartments using a recombinant CNG channel[12] and the FRET-based Epac2-camps sensor,[13] respectively. Changes in the cAMP level in these 2 compartments were compared in real time with the degree of PKA phosphorylation of $Ca_V1.2$ channels by monitoring the amplitude of $I_{Ca,L}$. Unlike most previous studies performed under steady-state conditions, here, we only used brief (15-second) β-AR stimulations, similar to those elicited during a startle response. This approach allowed us to follow in detail the onset and recovery phases for the 3 parameters and to delineate the intricate spatiotemporal contribution of PDE isoforms 3 and 4 to the β-AR response of cardiac myocytes.

Materials and Methods

All experiments performed conform to the European Community guiding principles in the care and use of animals (86/609/CEE, CE Off J no. L358, 18 December 1986), the local ethics committee (CREEA Ile-de-France Sud) guidelines, and the French decree no. 87-848 of October 19, 1987 (J Off République Française, 20 October 1987, pp 12245–12248). Authorizations to perform animal experiments according to this decree were obtained from the French Ministère de l'Agriculture, de la Pêche et de l'Alimentation (no. 92-283, June 27, 2007).

Detailed methods are included in the online data supplement at http://circres.ahajournlas.org.

Results

Compartmentalized cAMP and $I_{Ca,L}$ Responses to β-AR Stimulation

To compare β-adrenergic cAMP signals in the subsarcolemmal and cytosolic compartments, E583M/C460W CNGA2[14] and Epac2-camps[13] were expressed in ARVMs using recombinant adenoviruses. These sensors can detect rapid changes in cAMP with similar sensitivity ($EC_{50} \approx 1$ μmol/L).[13,14] Application of isoprenaline (Iso) (100 nmol/L) during a 15-second pulse produced a rapid and transient increase in cAMP at the plasma membrane, as monitored by the CNGA2 current density (dI_{CNG}; Figure 1A). As shown on the images in Figure 1B, cyan (CFP) and yellow (YFP) fluorescent protein fluorescence were uniform throughout cells expressing Epac2-camps, indicating cytosolic localization of the probe. The same 15-second Iso pulse elicited a transient rise of $[cAMP]_i$, as monitored by FRET changes between CFP and YFP (Figure 1B) and the consequent changes in CFP/YFP ratio (Figure 1C). With both sensors, cAMP detection occurred immediately after Iso application, confirming that β-AR and G_s activation occurred in less than 5 seconds.[4,15] As shown by the CFP/YFP ratio images in Figure 1C (also see the Movie in the online data supplement), Iso application produced a global increase of the cAMP signal, with no obvious striation pattern. Once produced, cAMP binds to tetrameric PKA, which dissociates into catalytic and regulatory subunits. Free catalytic subunits then phosphorylate various substrates, including the L-type Ca^{2+} channels. Figure 1D shows an example of $I_{Ca,L}$ increase elicited by a 15-second pulse of Iso, thus allowing to further compare cAMP kinetics with that of the phosphorylation of 1 of its final effectors. The average of several similar experiments measuring cAMP responses with the different indicators and $I_{Ca,L}$ potentiation are presented in Figure 2. Iso-induced subsarcolemmal cAMP transients led to dI_{CNG} that peaked at 10.7±1.6 pA/pF in t_{max}=38.3±3.1 seconds (Figure 2A and 2D) before returning rapidly to baseline (τ_{decay}=33.9±2.6 seconds, n=26; Figure 2E). In the cytosol, Iso elicited a maximal FRET variation of 9.1±0.5%, with a significantly slower time course than that measured at the plasma membrane by I_{CNG} (t_{max}=57.6±1.6 seconds and τ_{decay}=73.4±2.0 seconds, n=49; $P<0.001$ versus dI_{CNG} values; Figure 2B, 2D, and 2E). Thus, cAMP transients rise and decrease faster at the plasma membrane than in the cytosol. The responses of $[cAMP]_i$ to Iso in both compartments preceded that of $I_{Ca,L}$ (Figure 2C). The maximal increase in $I_{Ca,L}$ (+133.5±10.4%, n=18) occurred at t_{max}=82.2±5.4 seconds (n=18; $P<0.001$ versus t_{max} for I_{CNG}), and $I_{Ca,L}$ was still strongly enhanced when $[cAMP]_i$ had already returned to basal levels (τ_{decay}=259.2±34.8 seconds, $P<0.001$ versus I_{CNG}). This suggests that molecular events occurring downstream of cAMP are rate-limiting for both the rise and decay of $I_{Ca,L}$.

PDE Modulation of cAMP and $I_{Ca,L}$ Responses to β-AR Stimulation

$[cAMP]_i$ is tightly controlled by PDEs, with PDE3 and PDE4 contributing the majority of cAMP-PDE activity in rat cardiac myocytes.[8–10] Therefore, we examined the role of these 2 PDEs in regulating cAMP and $I_{Ca,L}$ signals in response to β-AR stimulation using the selective inhibitors cilostamide (Cil) (PDE3) and Ro 20-1724 (Ro) (PDE4), respectively. We showed previously that global PDE inhibition with 3-isobutyl-l-methylxanthine (IBMX) barely affected basal cAMP levels measured with CNG channels but strongly increased basal $I_{Ca,L}$.[8,16] This effect on $I_{Ca,L}$ could be reproduced by concomitant blockade of PDE3 and PDE4, whereas selective inhibition of a single PDE family was without effect.[16] We confirmed this finding here and characterized the effect of both inhibitors on basal cAMP monitored by Epac2-camps (see Figure I in the online data supplement). Application of Cil (1 μmol/L) or Ro (10 μmol/L) alone generally induced a slight (<0.5%) but significant increase of basal FRET ratio. Concomitant inhibition of PDE3 and PDE4 resulted in either a substantial cAMP elevation or, in some cells, had no effect. On average, Cil+Ro increased the FRET ratio by 4.3±1.86% (n=9). These results suggest a low and variable basal cAMP synthesis in ARVMs counterbalanced by PDE3 and PDE4.

We next determined the role of PDE4 in terminating β-AR stimulation (Figure 3). Incubation of ARVMs with Ro (10 μmol/L) before the Iso pulse increased the amplitude of

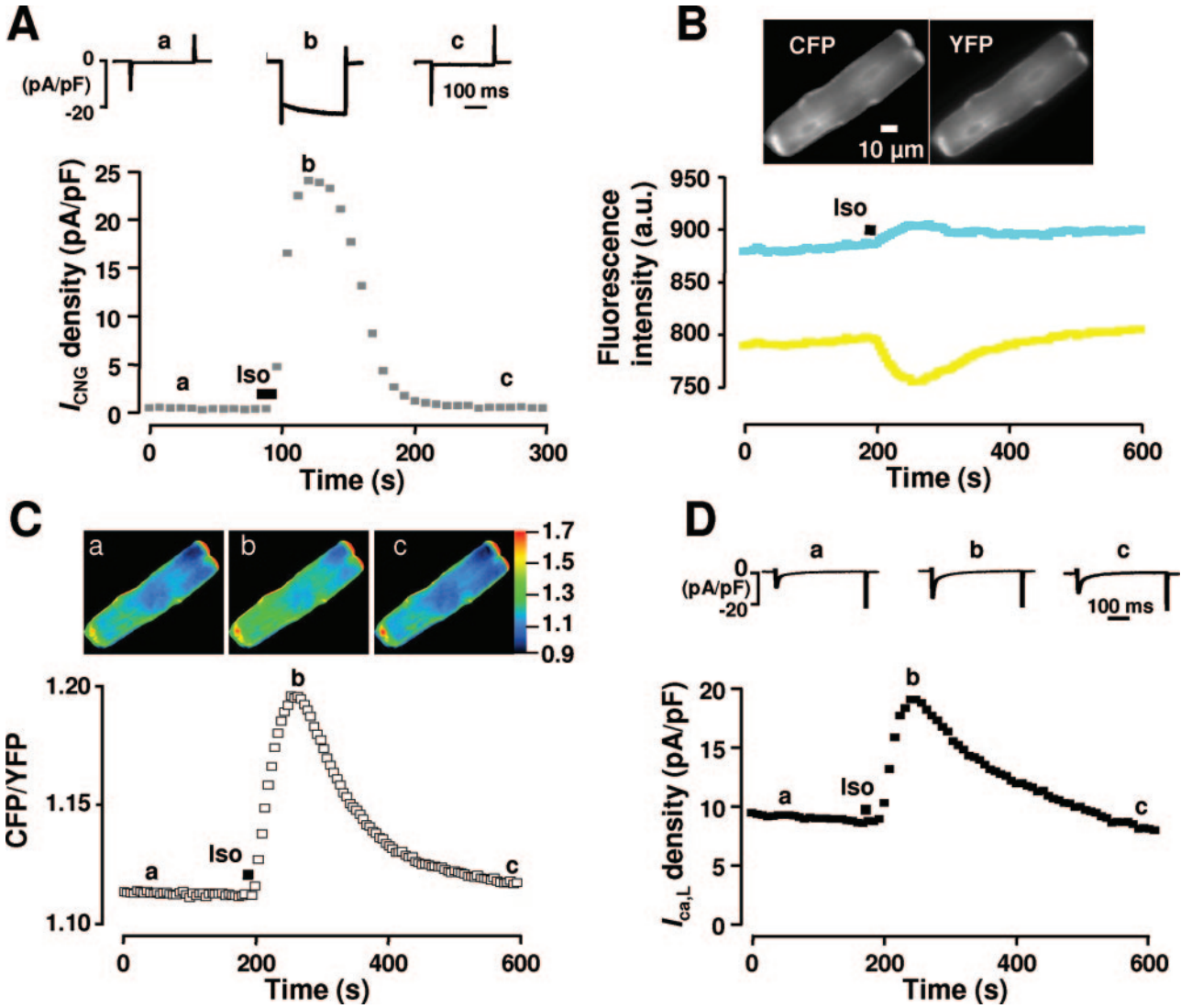

Figure 1. Real-time measurements of compartmentalized cAMP and $I_{Ca,L}$ responses to a transient β-AR stimulation in ARVMs. A, Representative cAMP signal monitored in an ARVM expressing C460W/E583M CNGA2 in response to a short application of Iso (100 nmol/L, 15 seconds). Each symbol on the lower graph represents the CNG current density (dI_{CNG}) measured every 8 seconds at −50 mV from a holding potential of 0 mV. The individual current traces shown on top were recorded at the times indicated by the corresponding letters in the graph below. B, Raw images of an ARVM infected with Epac2-camps adenovirus obtained on CFP excitation at 440±20 nm. The graph shows variations of CFP and YFP fluorescence emissions on Iso application as in A. Transient cAMP binding to the sensor induces a transient decrease in fluorescence resonance energy transfer (FRET) between CFP and YFP visualized by a simultaneous increase in donor emission (CFP, blue squares) and a decrease in acceptor emission (YFP, yellow squares). Acquisitions were performed every 5 seconds. C, Variation of the corrected CFP/YFP ratio (see Materials and Methods) in the same cell as in B. Pseudocolor images reflecting the CFP/YFP ratio were recorded at the times indicated by the letters on the graph below. All images show no apparent striation. D, Time course of $I_{Ca,L}$ in a cell stimulated as in A and B. Each square represents the amplitude of $I_{Ca,L}$ recorded every 8 seconds during a depolarization from −50 to 0 mV. The individual current traces shown on top were recorded at the times indicated by the corresponding letters in the graph below.

the cAMP response to Iso both at the membrane (by 88.9±3.3%, n=20; $P<0.05$ versus Iso alone; Figure 3A) and in the cytosol (by 58.0±7.9%, n=19; $P<0.001$ versus Iso alone; Figure 3B), along with an increase in the amplitude of the $I_{Ca,L}$ response (by 55.2±8.5%, n=12; $P<0.001$ versus Iso alone; Figure 3C). Ro also greatly prolonged the effect of Iso on cAMP in both the subsarcolemmal and cytosolic compartments by increasing the duration of the rising phases (t_{max}=84.2±9 seconds, n=20 for I_{CNG} and t_{max}=128.9±13.6 seconds, n=19 for the FRET signal; $P<0.001$ versus Iso alone for each; Figure 3D) and the duration of the decay phases (τ_{decay}=106.6±12.2 seconds for I_{CNG} and τ_{decay}=367.6±54.2 seconds for the FRET signal; $P<0.001$ versus Iso alone for each; Figure 3E). Ro had similar effects on $I_{Ca,L}$: time to peak and decay were significantly increased on PDE4 inhibition (t_{max}=129.3±10.2 seconds, $P<0.001$ and τ_{decay}=380.8±55.4 seconds, $P<0.05$ versus Iso alone, n=12). These results identify PDE4 as an essential regulator of β-AR cAMP signals and L-type Ca^{2+} channel in ARVMs.

In contrast, when PDE3 activity was inhibited using 1 μmol/L Cil, we detected only a slight, but significant, prolongation of the cAMP response at the plasma membrane (Figure 4A). Time to maximal I_{CNG} density was delayed (t_{max}=54.1±6.4 seconds, n=25, $P<0.01$) in the presence of

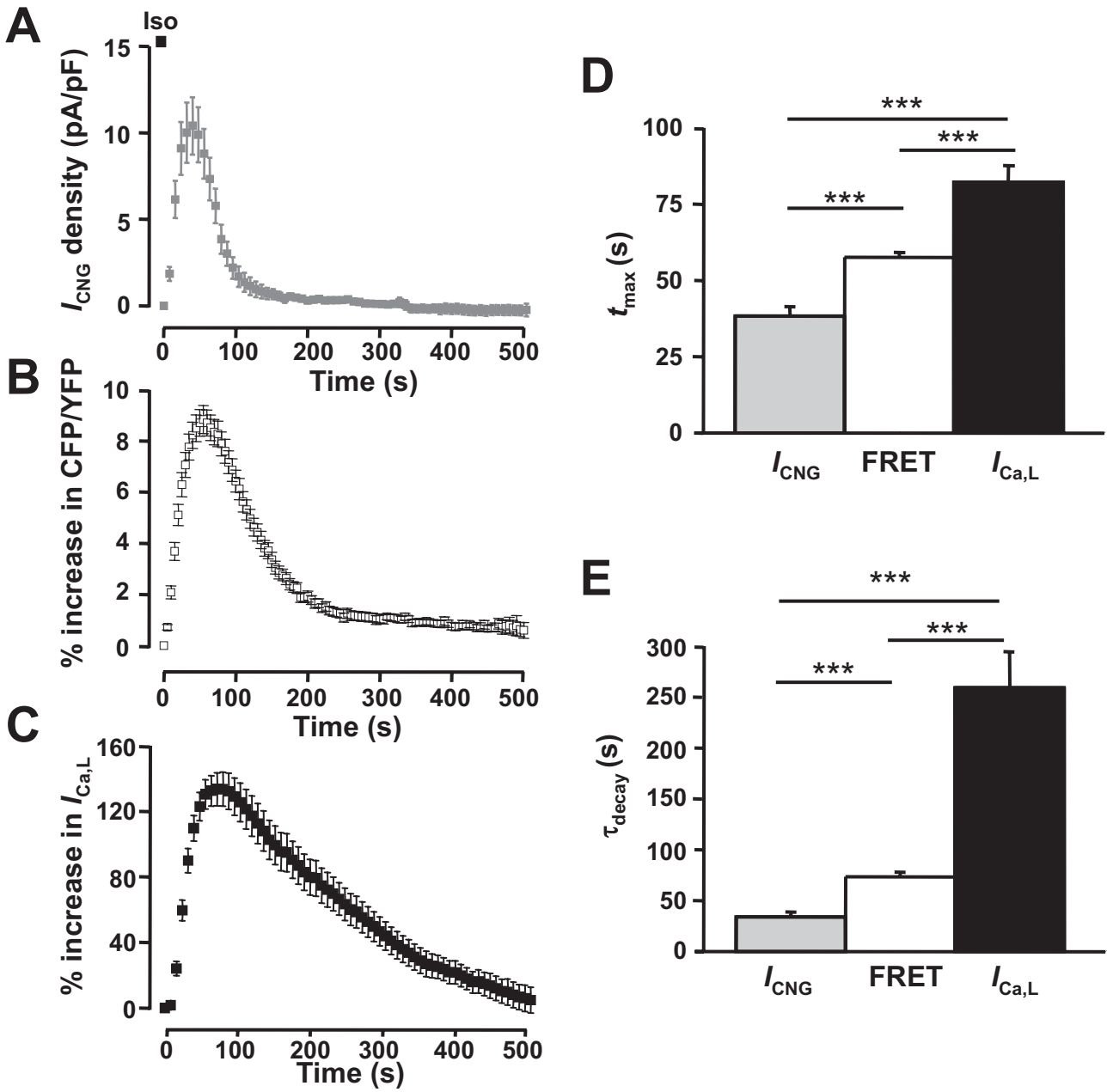

Figure 2. Comparative kinetics of subsarcolemmal cAMP, cytosolic cAMP, and $I_{Ca,L}$ responses to β-AR stimulation in ARVMs. Summary of several experiments performed as in Figure 1. A, Average time course of I_{CNG} density (n=27). B, Mean variation of CFP/YFP ratio measured by Epac2-camps (n=49). C, Mean variation of $I_{Ca,L}$ amplitude (n=18). D and E, Kinetic parameters t_{max} and τ_{decay} for I_{CNG} (gray bar), CFP/YFP ratio (white bar), and $I_{Ca,L}$ (black bar). ***Statistically significant differences ($P<0.001$).

the inhibitor (Figure 4A and 4D), but the maximal amplitude (13.5±1.8 pA/pF) and the rate of decay (τ_{decay}=37.8±2.7 seconds, Figure 4E) were not significantly different from the control values obtained with Iso alone. Moreover, Cil did not affect Iso-induced cytosolic cAMP signals or $I_{Ca,L}$ (Figure 4B through 4E). In the presence of Cil, the FRET ratio increased by 9.7±0.9% (n=18) on an Iso challenge, with similar kinetics as in control (t_{max}=59.2±2.0 seconds and τ_{decay}=63.6±2.5 seconds). Similarly, Cil neither modified the amplitude (164.0±14.5% increase over control, n=13) nor the time course (t_{max}=75.0±6.5 seconds and τ_{decay}=272.2±42.5 seconds) of the Iso increase of $I_{Ca,L}$.

These results suggest that PDE3 plays a minor role in the regulation of cAMP and $I_{Ca,L}$ responses to a brief β-AR stimulation in ARVMs. Yet, other PDE(s) besides PDE4 must be involved in degrading β-AR-dependent cAMP because I_{CNG} density and FRET ratio still declined in the presence of Ro (Figure 3). To determine whether the remaining PDE activity after PDE4 blockade was attributable to PDE3, the cells were preincubated with Ro (10 μmol/L) during 2 minutes, then Cil (1 μmol/L) was added together with Iso. After 15 seconds, Iso was washed out in the continuous presence of Cil and Ro. As shown in Figure 5A through 5C, simultaneous inhibition of PDE3 and PDE4 did

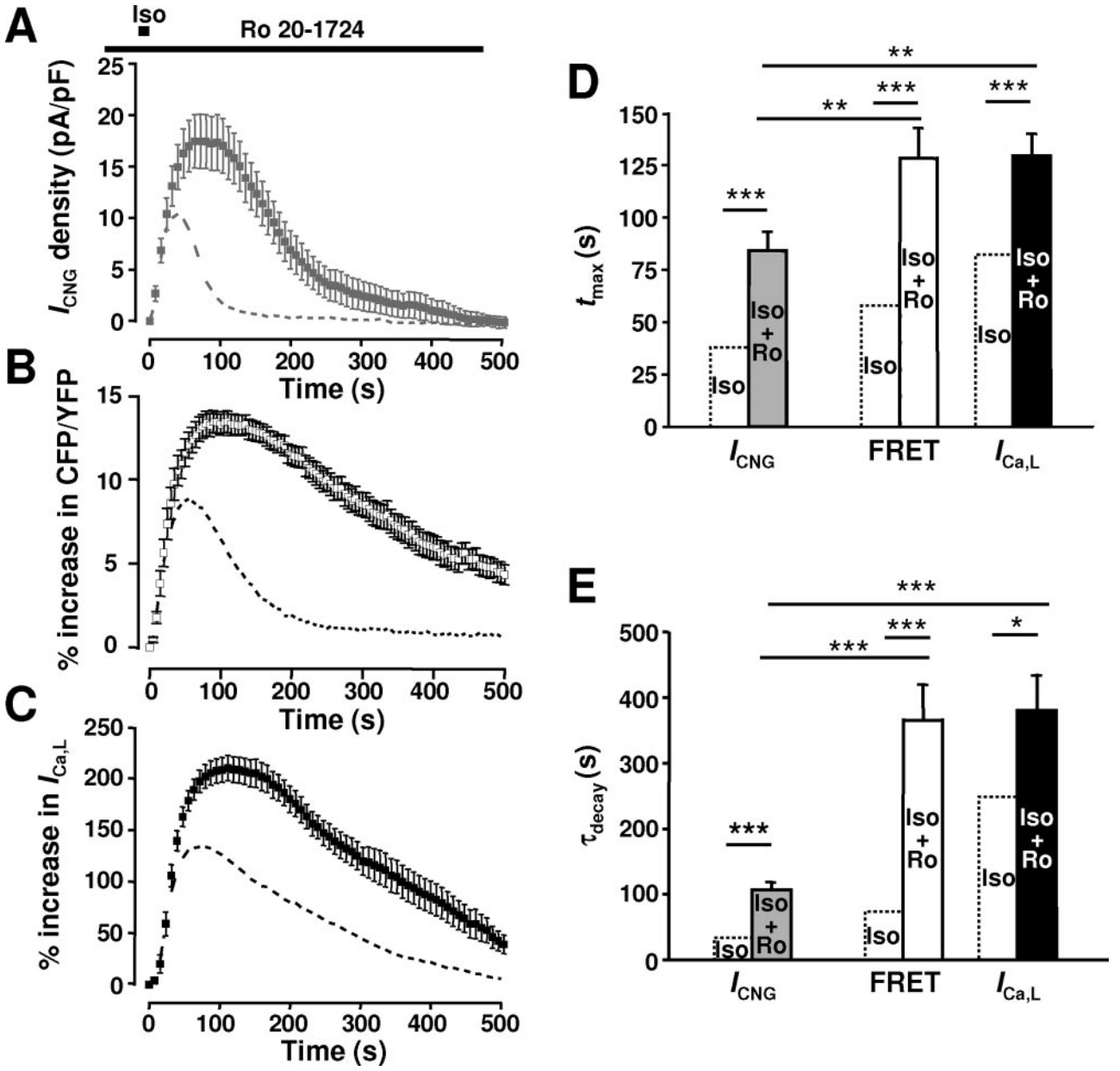

Figure 3. PDE4 modulates β-AR responses in ARVMs. Cells were exposed to the PDE4 inhibitor Ro (10 μmol/L) 2 minutes before the 15-second pulse of Iso (100 nmol/L) and then maintained throughout the experiments. All graphs represent the means(±SEM) and show the time course of I_{CNG} density (n=20) (A) and the percentage increase in CFP/YFP ratio (n=19) (B) and of $I_{Ca,L}$ (n=12) (C) elicited by Iso in the presence of Ro. Dashed lines indicate the effect of Iso alone as in Figure 2. D and E show the means(±SEM) of t_{max} and τ_{decay} obtained from experiments shown in A through C. For comparison, the dashed bars represent the corresponding parameters obtained with Iso alone (taken from Figure 2D and E). Statistically significant differences are indicated as: $^{*}P<0.05$; $^{**}P<0.01$; $^{***}P<0.001$.

not further increase the amplitude of Iso-dependent responses compared with Ro alone (dI_{CNG} was increased to 15.3±2.0 pA/pF, n=13; the FRET ratio was increased by 12.3±0.6%, n=10, and $I_{Ca,L}$ was potentiated by 191.4±21.2%, n=10 in the presence of Cil+Ro). The values for t_{max} obtained in these conditions were similar to those obtained when only PDE4 was blocked (Figure 3) most likely because, unlike in Figure 4, PDE3 was not fully inhibited during the rising phase of the Iso response. However, we observed a considerable prolongation of Iso-triggered responses, so that the rates of decay could not be accurately estimated by exponential fitting over a period of 500 seconds. Thus, even though PDE3 inhibition alone had almost no effect on any parameters, PDE3 activity was sufficient to terminate β-AR–dependent cAMP and $I_{Ca,L}$ responses when PDE4 was inhibited. We tested the participation of additional PDEs by including the wide spectrum PDE inhibitor IBMX (300 μmol/L) during the Iso stimulation and washout. The effect of IBMX was similar to that of Cil+Ro on membrane cAMP (dI_{CNG}) and $I_{Ca,L}$ (Figure 5A and 5C). In contrast, IBMX suppressed the residual cAMP decrease in the cytosol (Figure 5B), suggesting that other PDEs, such as PDE1 and PDE2, are active in this compartment. The IBMX-resistant, slow decrease in I_{CNG} density and $I_{Ca,L}$ likely reflects cAMP diffusion from the membrane compartment to

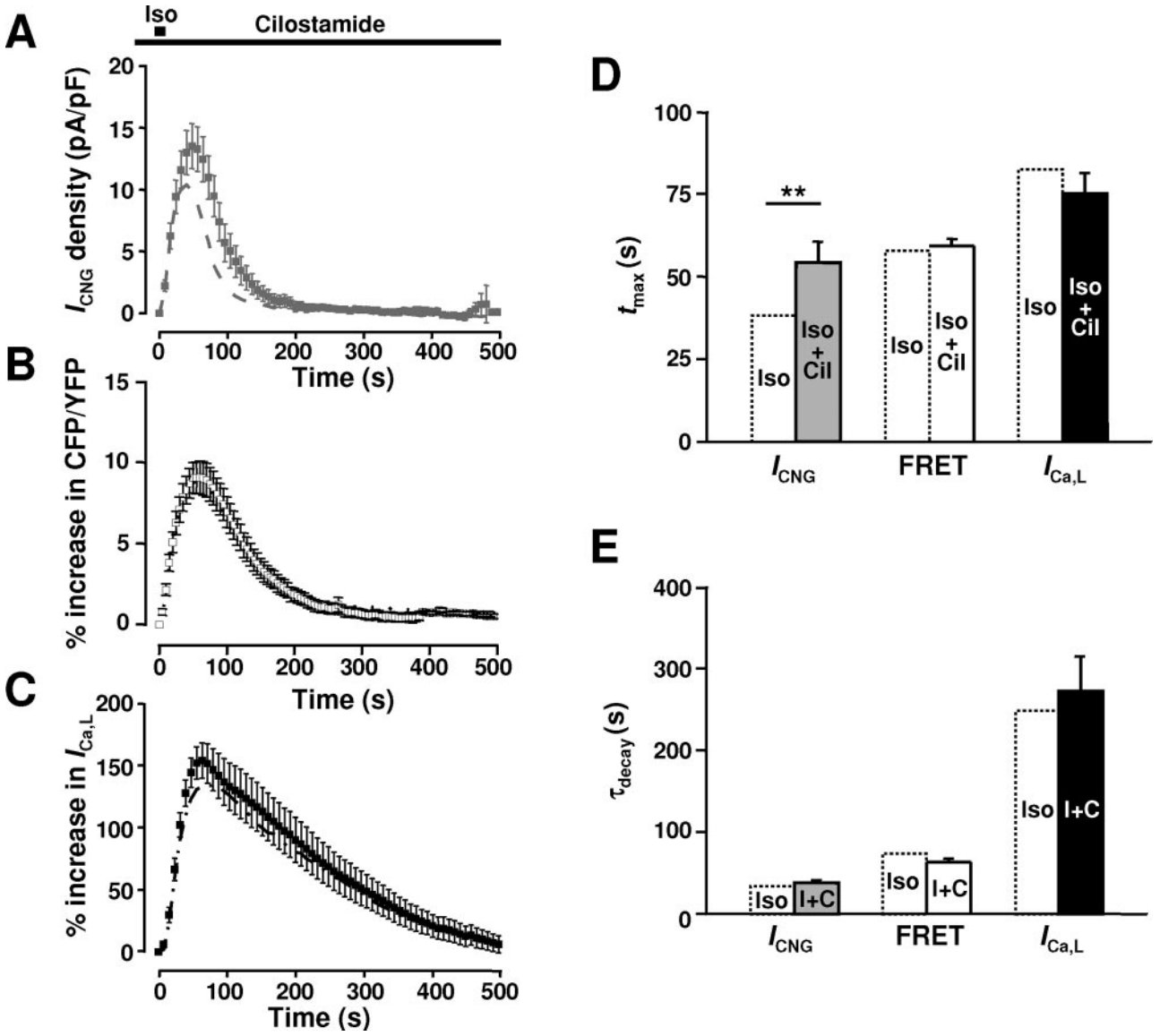

Figure 4. Effect of PDE3 inhibition on β-AR responses in ARVMs. Cells were exposed to the PDE3 inhibitor Cil (1 μmol/L) 2 minutes before the 15-second Iso pulse (100 nmol/L) and throughout the rest of the experiments. Graphs represent the means(±SEM) time course of I_{CNG} density (n=25) (A), CFP/YFP ratio (n=18) (B), and $I_{Ca,L}$ (n=13) (C) after Iso treatment in the presence of Cil. Dashed lines represent the effect of Iso alone as presented in Figure 2. cAMP transients measured by CNG channels (A) were significantly slowed by PDE3 inhibition. D and E, Kinetic parameters t_{max} and τ_{decay} for I_{CNG} (gray bars), FRET ratio (white bar), and $I_{Ca,L}$ (black bar). For comparison, the dashed bars represent the corresponding parameters obtained with Iso alone (taken from Figure 2D and 2E).

the cytosol dialyzed by the internal patch pipette solution.[12] However, the rate of dI_{CNG} decrease in the presence of IBMX was approximately 1 order of magnitude smaller than the rate of dI_{CNG} decrease without IBMX, making cAMP leak through the patch pipette a negligible contributor of dI_{CNG} kinetics in the previous experimental conditions.

PKA-Mediated PDE4 Activation Regulates β-AR cAMP Signals in ARVMs

Using CNG channels, we have shown previously that subsarcolemmal cAMP signals are controlled by a negative feedback involving PKA activation of PDE3 and PDE4.[8] Coexpression of Epac2-camps with rabbit muscle cAMP-dependent protein kinase inhibitor (PKI)[17] allowed us to examine the role of PKA in cytosolic cAMP degradation. As shown in Figure 6A through 6C, PKI overexpression increased the amplitude (by 58.9±9.6%, n=26; $P<0.001$ versus Iso alone) and duration (t_{max}=91.0±6.3 seconds and τ_{decay}=123.9±3.4 seconds, n=26; $P<0.001$ versus Iso alone) of the FRET response to Iso. Additional PDE4 inhibition further slowed the cAMP signal detected by the FRET sensor, but we obtained a similar time course as with Ro alone (see Figure 3B, 3D, and 3E). Thus, PKI had no additional effect over PDE4 inhibition, suggesting that PKA regulation of β-AR cAMP levels in the cytosol of ARVMs is mainly attributable to PDE4 activation. We tested whether this mechanism could mask the participation of PDE3. In the presence of PKI, Cil had a small but significant effect on the decay phase of Iso-induced cAMP (Figure 6A through 6C). The fact that Cil had a much larger effect in the presence of

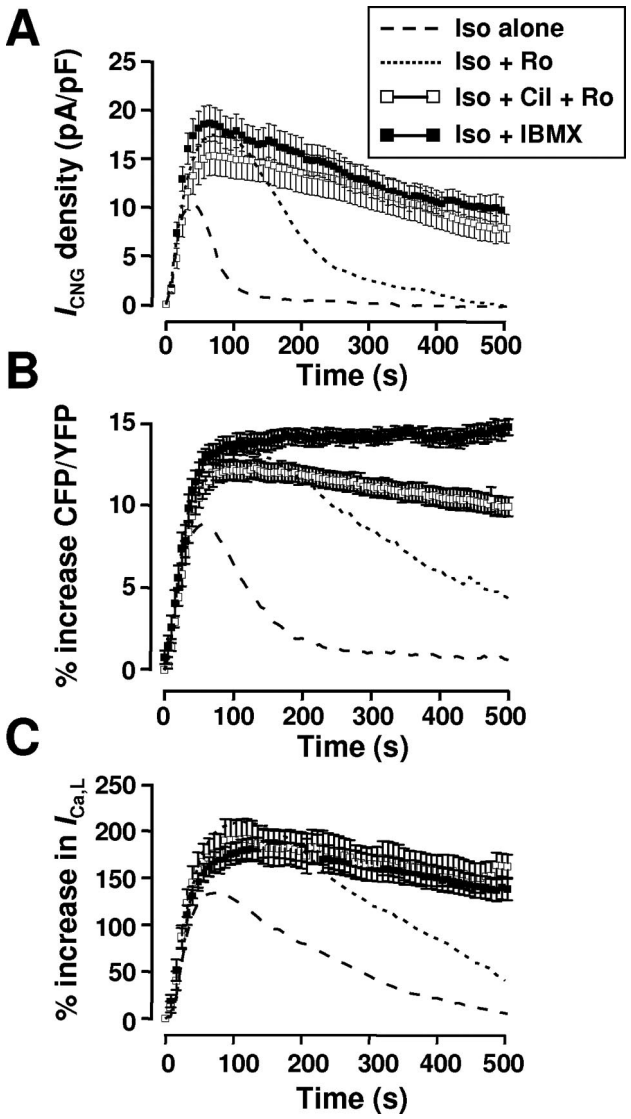

Figure 5. PDE4 inhibition unmasks PDE3 activity in ARVMs. ARVMs were superfused with Ro (10 μmol/L) for 2 minutes before the 15-second pulse of Iso. Cil and Ro were added to the Iso solution and in the washout solution to achieve selective inhibition of PDE3 and PDE4 (empty squares) or were replaced by IBMX (300 μmol/L) to block all PDEs (black squares). The dashed line represents the effect of Iso alone and the dotted line in the presence of Ro, as presented in Figure 3. A, I_{CNG} density in the presence of Ro and Cil (n=13) or IBMX (n=14). B, CFP/YFP ratio in the presence of Ro and Cil (n=10) or IBMX (n=10). C, $I_{Ca,L}$ in the presence of Ro and Cil (n=10) or IBMX (n=6). All graphs represent the means±SEM of the number of independent experiments indicated.

Ro (Figure 5B), which fully blocks PDE4 activity, than with PKI, which only prevents its activation by PKA,[18] suggests that basal PDE4 activity is sufficient to hydrolyze most of the cAMP produced by β-AR stimulation even when PDE3 is inhibited. This hypothesis was confirmed in subsequent biochemical experiments (Figure 6D and 6E). Total cAMP hydrolytic activity was measured from homogenates of isolated cardiomyocytes, and specific PDE3 and PDE4 activities were determined using selective inhibitors. As shown in Figure 6D, total basal PDE activity was 99.4±8.29 pmol/min per milligram of protein, of which >60% was attributable to PDE4 (62.1±5.5 pmol/min per milligram of protein) and 30% to PDE3 (33.2±2.8 pmol/min per milligram of protein, n=10). Application of Iso (100 nmol/L, 15 seconds) increased total cAMP-hydrolytic activity by 47.0±4.4% (n=8, $P<0.01$ versus basal), and this was mainly attributable to PDE4 activation (by 69.4±7.3%, n=8; $P<0.01$), although there was also a small increase in PDE3 activity (by 35.6±6.4%, n=8; $P<0.05$). Furthermore, this activation was dependent on the level of β-AR stimulation (Figure 6E), suggesting that the level of PDE activation follows cAMP elevation induced by β-AR agonists.

Discussion

In the present study, we determined the kinetics of β-AR–induced cAMP signals in different subcellular compartments of ARVMs using real-time cAMP sensors and compared them with the activation of an endogenous downstream target of cAMP/PKA signaling, $I_{Ca,L}$. We also evaluated the contribution of PDEs to the regulation of these signaling events. The main findings were as follows: (1) submembrane and cytosolic cAMP signals display different kinetics, indicating a restricted cAMP diffusion between these compartments; (2) $I_{Ca,L}$ stimulation develops >2-fold slower, and its return to basal levels develops >7-fold slower compared with membrane cAMP responses, suggesting that $Ca_v1.2$ phosphorylation and dephosphorylation are rate-limiting in the β-AR cascade; (3) PDE4 is the main PDE subtype modulating β-AR cAMP transients and, as a consequence, $I_{Ca,L}$ recovery after β-AR stimulation; (4) PKA shapes β-AR cAMP transients by activating PDE4; and (5) β-AR cAMP signals are differentially regulated by PDEs at the membrane and in the cytosol.

Although several recent studies investigated cAMP signaling and compartmentation of cyclic nucleotides using live-cell imaging in cardiac cells, most of these were performed using neonatal cells.[4,6,9] Because subcellular structures may play an important role in cAMP compartmentation, we used highly differentiated adult cardiac myocytes in the present study. Despite the presence of developed T-tubular network in ARVMs, fluorescence images of Epac2-camps probe showed no obvious striated pattern on the ratio images in either quiescent cells or following β-AR stimulation. This contrasts with the result of a previous report where a cAMP sensor developed on the basis of the R and C subunits of PKA did show striated cAMP patterns[6] but corroborates subsequent studies using other FRET-based cAMP sensors[7] and A-kinase activity reporter (AKAR2).[4]

Following a 15-second Iso pulse, cAMP transients in both subsarcolemmal and cytosolic compartments started almost immediately after Iso application, in agreement with earlier estimates of the kinetics of the β-AR/G_s/adenylyl cyclase cascade.[4,15] However, comparing the CNG current with the Epac2-camps signal showed that cAMP kinetics (rise and decay) were faster at the membrane than in the cytosol. These kinetics were too fast to be notably influenced by cAMP diffusion in the patch pipette (as estimated from measurements with IBMX, see also Rich et al[12]). Also, I_{CNG} and Epac2-camps have a similar sensitivity to cAMP ($K_D \approx 1$ μmol/L),[13,14] and the binding and dissociation kinetics

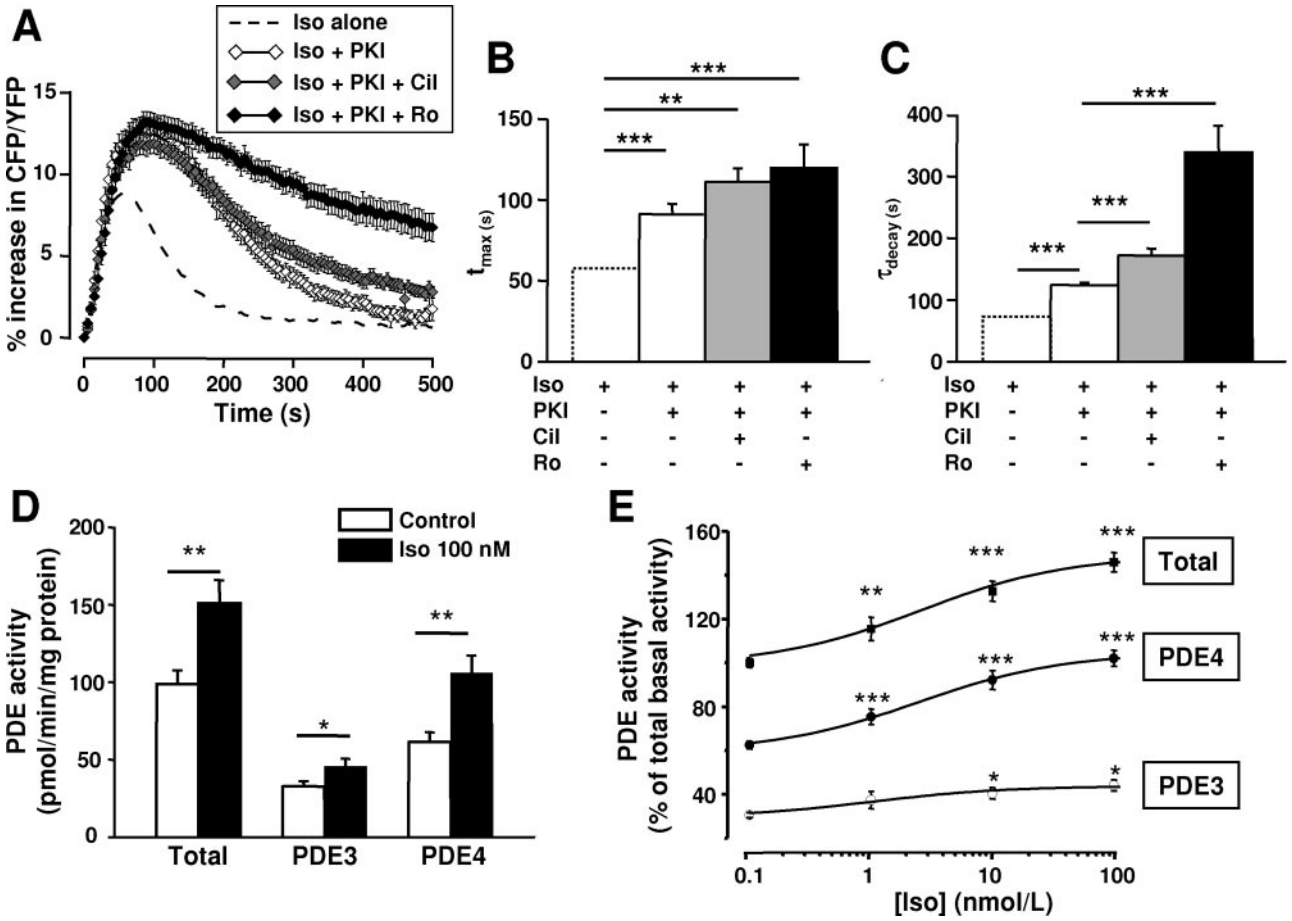

Figure 6. PKA activation of PDE3 and PDE4 is involved in the β-AR control of cytosolic cAMP in ARVMs. A, Effect of a 15-second pulse of Iso (100 nmol/L) in ARVMs coexpressing Epac2-camps and PKI without PDE inhibitors (white diamonds, n=26), in the presence of 1 μmol/L Cil (gray diamonds, n=29) or 10 μmol/L Ro (black diamonds, n=19). Dashed line represents the effect of Iso in the absence of PKI (such as presented in Figure 1B). B and C, Bar graphs summarizing the effect of PKI (empty bars), PKI+Cil (gray bars), and PKI+Ro (black bars) on the kinetic parameters t_{max} (B) and τ_{decay} (C) of the CFP/YFP ratio. D, Total, PDE3, and PDE4 activities in ARVMs before (white bars, n=10) and after a 15-second pulse of Iso (100 nmol/L, black bars, n=8). E, Concentration–response curves to Iso for total PDE activity (black squares), PDE3 activity (empty circles), and PDE4 activity (black circles) in n=6 to 8 experiments. PDE activities are represented as a percentage of total basal PDE activity. All graphs represent the means±SEM and statistical significance is indicated as: *$P<0.05$; **$P<0.01$; ***$P<0.001$.

of cAMP on the 2 sensors are much faster than the measured kinetics during Iso response (see the online data supplement for details). Thus, β-AR stimulation of ARVMs leads to cAMP signals with different dynamics in distinct compartments, as previously reported in HEK-293 cells.[19–21] The cytosolic versus membrane cAMP signals described here were delayed to the same extent as recently reported for cytosolic versus membrane PKA activity using AKAR2 sensors in neonatal cardiomyocytes.[4] Such synchronization indicates that a cAMP gradient between membrane and cytosol creates a phosphorylation gradient mediated by PKA in cardiac cells. As noted previously,[4,21] the delay between membrane and cytosolic cAMP-mediated events is not compatible with cAMP diffusion rates measured in the cytosol.[7] Thus, cAMP diffusion from the membrane to the bulk cytosol must be restricted either by an enzymatic or a physical barrier.[12,22]

The rate of $I_{Ca,L}$ stimulation reported here is similar to those reported earlier for $I_{Ca,L}$ in frog ventricular myocytes,[23] for neuronal potassium channels,[24] and for the membrane-associated PKA sensor AKAR2.[4] Activation of $Ca_v1.2$ developed >2-times slower than the rise of cAMP at the membrane, suggesting that the rate-limiting step in the β-AR stimulation of $I_{Ca,L}$ occurs after cAMP accumulation. This is likely attributable to PKA activation, as suggested by the slower response of the PKA-based cAMP probe, FlCRhR, to β-AR stimulation in frog ventricular myocytes.[23] The recovery of $I_{Ca,L}$ from β-AR stimulation was also comparable to previous results in frog cells[23] and to dephosphorylation kinetics of AKAR2.[4] The considerable delay between $I_{Ca,L}$ recovery and cAMP decay indicates that mechanisms other than cAMP degradation by PDEs are rate-limiting in the recovery of $I_{Ca,L}$: these include the deactivation of PKA, dephosphorylation of the L-type Ca^{2+} channel by phosphatases, or recovery of basal Ca^{2+} channel gating.[23]

The rapid decay of I_{CNG} compared to Epac2-camps signal could be attributable to diffusion of cAMP to the cytosol and degradation by PDEs. PDEs have been shown to be localized at the plasma membrane through membrane-association domains (such as PDE3[25]) or protein–protein interactions[26,27]

and are more concentrated at the plasma membrane than in the cytosol.[28] Differential cAMP degradation might lead to faster phosphorylation/dephosphorylation of membrane proteins (such as the calcium channels) as compared with cytosolic proteins on a given stimulus, as previously suggested in neurons.[24]

A number of previous studies demonstrated that basal cAMP levels are controlled by PDEs in resting cardiac cells.[6,9,10,16,29] Basal cAMP turnover is mainly regulated by PDE4 in neonatal cardiomyocytes,[9] whereas both PDE3 and PDE4 regulate resting cAMP levels and $I_{Ca,L}$ in adult cells.[16] We previously reported that IBMX had no effect on subsarcolemmal cAMP levels measured with CNG channels in ARVMs.[8] Here, using Epac2-camps, we detected a variable but significant increase in basal cAMP on PDE3 and PDE4 inhibition (supplemental Figure I). Because both sensors present similar affinities for cAMP[13,14] but are located in distinct subcellular compartments, this result suggests that basal cAMP levels are different in distinct parts of the cell. This could be related to the presence of IBMX insensitive PDE8[30] or cAMP transporters such as multidrug resistance protein 5,[31] both of which are expressed in heart and might lower cAMP selectively at the membrane. Following β-AR stimulation, we confirm here that PDE4 is the main PDE degrading cAMP in ARVMs[7–9] and is crucial for Ca^{2+} channel regulation.[16] Interestingly, PDE4 inhibition had a more drastic effect on cytosolic cAMP than subsarcolemmal cAMP, in agreement with a major fraction of PDE4 activity being cytosolic in the rat myocardium.[32] Furthermore, inhibition of all PDE activities with IBMX had no additional effect at the membrane compared to simultaneous inhibition of PDE3 and PDE4, whereas it further delayed the decay of cytosolic cAMP signals (Figure 5B), suggesting that other PDEs, such as PDE1 or PDE2, are contributing to cAMP degradation in the cytosol.[10] In contrast, inhibition of PDE3 had only a minor effect on I_{CNG} and no effect on the FRET signal or $I_{Ca,L}$. These results are in agreement with previous studies in rodent cardiac myocytes[7,9] and may indicate a preferential location of PDE3 at the membrane.[25] However, when PDE4 was inhibited, PDE3 became predominant to hydrolyze membrane and cytosolic cAMP, as well as regulating $I_{Ca,L}$ recovery. Thus, it appears that PDE4 is able to compensate for PDE3 inhibition, at least in the cytosol and in the vicinity of L-type Ca^{2+} channels. This could be related to integration of PDE4 into A kinase anchoring protein–organized signaling complexes,[3,33] hence facilitating activation of PDE4 by PKA.[3,8,18] This mechanism is supported by the fact that PKA inhibition mimics, to some extent, the effect of Ro on cytosolic cAMP and that PDE4 activity is enhanced on β-AR stimulation.[8]

More generally, these results raise the question of the respective roles of PDE3 and PDE4 in regulating cardiac contractility in larger mammals, where PDE3 is thought to be predominant. This idea is based mainly on the fact that PDE3 inhibitors, contrary to PDE4 inhibitors, have a direct inotropic effect on basal contractility. However, PDE4 inhibitors exert strong inotropic responses in the presence of β-AR tone.[32] Thus, it is tempting to speculate that PDE3 regulates a "constitutive" cAMP pool linked to contractility, whereas PDE4 regulates the cAMP microdomains mobilized by β-AR stimulation. Further experiments in large mammals and humans are necessary to verify this hypothesis.

Acknowledgments

We are indebted to Florence Lefebvre for superb technical assistance. We thank Valérie Domergue-Dupont and the animal core facility of IFR141 for efficient handling and preparation of the animals. We are also grateful to Dr Hazel Lum (University of Illinois, Chicago) for providing us the adenovirus encoding PKI, Dr Dermot Cooper (University of Cambridge, UK) for the adenovirus encoding CNGA2 mutants, and Drs Stefan Engelhardt and Martin Lohse (University of Würzburg, Germany) for the adenovirus encoding Epac2-camps.

Sources of Funding

This work was supported by grants from the Fondation Leducq 06CVD02 cycAMP (to R.F. and M.C.), European Union contract LSHM-CT-2005-018833/EUGeneHeart (to R.F.), the Fondation de France (to G.V.), and NIH grant HD20788 (to M.C.). A.A.-G. was a recipient of doctoral grants from the French Ministry of Education and Research and the Groupe de Réflexion sur la Recherche Cardiovasculaire. J.L. was recipient of a post doctoral grant from Fondation Lefoulon Delalande and Fondation pour la Recherche Médicale.

Disclosures

None.

References

1. Bers DM. Cardiac excitation-contraction coupling. *Nature*. 2002;415:198–205.
2. Steinberg SF, Brunton LL. Compartmentation of G protein-coupled signaling pathways in cardiac myocytes. *Ann Rev Pharmacol Toxicol*. 2001;41:751–773.
3. Dodge-Kafka KL, Langeberg L, Scott JD. Compartmentation of cyclic nucleotide signaling in the heart: the role of A-kinase anchoring proteins. *Circ Res*. 2006;98:993–1001.
4. Saucerman JJ, Zhang J, Martin JC, Peng LX, Stenbit AE, Tsien RY, McCulloch AD. Systems analysis of PKA-mediated phosphorylation gradients in live cardiac myocytes. *Proc Natl Acad Sci U S A*. 2006;103:12923–12928.
5. Jurevicius J, Fischmeister R. cAMP compartmentation is responsible for a local activation of cardiac Ca^{2+} channels by β-adrenergic agonists. *Proc Natl Acad Sci U S A*. 1996;93:295–299.
6. Zaccolo M, Pozzan T. Discrete microdomains with high concentration of cAMP in stimulated rat neonatal cardiac myocytes. *Science*. 2002;295:1711–1715.
7. Nikolaev VO, Bunemann M, Schmitteckert E, Lohse MJ, Engelhardt S. Cyclic AMP imaging in adult cardiac myocytes reveals far-reaching β_1-adrenergic but locally confined β_2-adrenergic receptor-mediated signaling. *Circ Res*. 2006;99:1084–1091.
8. Rochais F, Vandecasteele G, Lefebvre F, Lugnier C, Lum H, Mazet J-L, Cooper DMF, Fischmeister R. Negative feedback exerted by PKA and cAMP phosphodiesterase on subsarcolemmal cAMP signals in intact cardiac myocytes. An *in vivo* study using adenovirus-mediated expression of CNG channels. *J Biol Chem*. 2004;279:52095–52105.
9. Mongillo M, McSorley T, Evellin S, Sood A, Lissandron V, Terrin A, Huston E, Hannawacker A, Lohse MJ, Pozzan T, Houslay MD, Zaccolo M. Fluorescence resonance energy transfer-based analysis of cAMP dynamics in live neonatal rat cardiac myocytes reveals distinct functions of compartmentalized phosphodiesterases. *Circ Res*. 2004;95:65–75.
10. Rochais F, Abi-Gerges A, Horner K, Lefebvre F, Cooper DMF, Conti M, Fischmeister R, Vandecasteele G. A specific pattern of phosphodiesterases controls the cAMP signals generated by different G_s-coupled receptors in adult rat ventricular myocytes. *Circ Res*. 2006;98:1081–1088.
11. Fischmeister R, Castro LRV, Abi-Gerges A, Rochais F, Jurevicius J, Leroy J, Vandecasteele G. Compartmentation of cyclic nucleotide signaling in the heart: the role of cyclic nucleotide phosphodiesterases. *Circ Res*. 2006;99:816–828.

12. Rich TC, Fagan KA, Nakata H, Schaack J, Cooper DMF, Karpen JW. Cyclic nucleotide-gated channels colocalize with adenylyl cyclase in regions of restricted cAMP diffusion. *J Gen Physiol*. 2000;116:147–161.
13. Nikolaev VO, Bunemann M, Hein L, Hannawacker A, Lohse MJ. Novel single chain cAMP sensors for receptor-induced signal propagation. *J Biol Chem*. 2004;279:37215–37218.
14. Rich TC, Tse TE, Rohan JG, Schaack J, Karpen JW. In vivo assessment of local phosphodiesterase activity using tailored cyclic nucleotide-gated channels as cAMP sensors. *J Gen Physiol*. 2001;118:63–77.
15. Frace AM, Méry P-F, Fischmeister R, Hartzell HC. Rate-limiting steps in the β-adrenergic stimulation of cardiac calcium current. *J Gen Physiol*. 1993;101:337–353.
16. Verde I, Vandecasteele G, Lezoualc'h F, Fischmeister R. Characterization of the cyclic nucleotide phosphodiesterase subtypes involved in the regulation of the L-type Ca^{2+} current in rat ventricular myocytes. *Br J Pharmacol*. 1999;127:65–74.
17. Lum H, Jaffe HA, Schulz IT, Masood A, RayChaudhury A, Green RD. Expression of PKA inhibitor (PKI) gene abolishes cAMP-mediated protection to endothelial barrier dysfunction. *Am J Physiol*. 1999;277:C580–C588.
18. Sette C, Conti M. Phosphorylation and activation of a cAMP-specific phosphodiesterase by the cAMP-dependent protein kinase-involvement of serine 54 in the enzyme activation. *J Biol Chem*. 1996;271:16526–16534.
19. Rich TC, Fagan KA, Tse TE, Schaack J, Cooper DM, Karpen JW. A uniform extracellular stimulus triggers distinct cAMP signals in different compartments of a simple cell. *Proc Natl Acad Sci U S A*. 2001;98:13049–13054.
20. Dipilato LM, Cheng X, Zhang J. Fluorescent indicators of cAMP and Epac activation reveal differential dynamics of cAMP signaling within discrete subcellular compartments. *Proc Natl Acad Sci U S A*. 2004;101:16513–16518.
21. Terrin A, Di Benedetto G, Pertegato V, Cheung YF, Baillie G, Lynch MJ, Elvassore N, Prinz A, Herberg FW, Houslay MD, Zaccolo M. PGE1 stimulation of HEK293 cells generates multiple contiguous domains with different [cAMP]: role of compartmentalized phosphodiesterases. *J Cell Biol*. 2006;175:441–451.
22. Warrier S, Ramamurthy G, Eckert RL, Nikolaev VO, Lohse MJ, Harvey RD. cAMP microdomains and L-type Ca^{2+} channel regulation in guinea-pig ventricular myocytes. *J Physiol*. 2007;580:765–776.
23. Goaillard JM, Vincent PV, Fischmeister R. Simultaneous measurements of intracellular cAMP and L-type Ca^{2+} current in single frog ventricular myocytes. *J Physiol*. 2001;530:79–91.
24. Gervasi N, Hepp R, Tricoire L, Zhang J, Lambolez B, Paupardin-Tritsch D, Vincent P. Dynamics of protein kinase A signaling at the membrane, in the cytosol, and in the nucleus of neurons in mouse brain slices. *J Neurosci*. 2007;27:2744–2750.
25. Wechsler J, Choi YH, Krall J, Ahmad F, Manganiello VC, Movsesian MA. Isoforms of cyclic nucleotide phosphodiesterase PDE3A in cardiac myocytes. *J Biol Chem*. 2002;277:38072–38078.
26. Baillie GS, Sood A, McPhee I, Gall I, Perry SJ, Lefkowitz RJ, Houslay MD. β-Arrestin-mediated PDE4 cAMP phosphodiesterase recruitment regulates β-adrenoceptor switching from G_s to G_i. *Proc Natl Acad Sci U S A*. 2003;100:941–945.
27. Richter W, Day P, Agraval R, Bruss MD, Granier S, Wang YL, Rasmussen SGF, Horner K, Wang P, Lei T, Patterson AJ, Kobilka BK, Conti M. Signaling from β_1- and β_2-adrenergic receptors is defined by differential interactions with PDE4. *EMBO J*. 2008;27:384–393.
28. Okruhlicova L, Tribulova N, Eckly A, Lugnier C, Slezak J. Cytochemical distribution of cyclic AMP-dependent 3′,5′-nucleotide phosphodiesterase in the rat myocardium. *Histochem J*. 1996;28:165–172.
29. Warrier S, Belevych AE, Ruse M, Eckert RL, Zaccolo M, Pozzan T, Harvey RD. β-Adrenergic and muscarinic receptor induced changes in cAMP activity in adult cardiac myocytes detected using a FRET based biosensor. *Am J Physiol Cell Physiol*. 2005;289:C455–C461.
30. Soderling SH, Bayuga SJ, Beavo JA. Cloning and characterization of a cAMP-specific cyclic nucleotide phosphodiesterase. *Proc Natl Acad Sci U S A*. 1998;95:8991–8996.
31. Dazert P, Meissner K, Vogelgesang S, Heydrich B, Eckel L, Bohm M, Warzok R, Kerb R, Brinkmann U, Schaeffeler E, Schwab M, Cascorbi I, Jedlitschky G, Kroemer HK. Expression and localization of the multidrug resistance protein 5 (MRP5/ABCC5), a cellular export pump for cyclic nucleotides, in human heart. *Am J Pathol*. 2003;163:1567–1577.
32. Weishaar RE, Kobylarz-Singer DC, Steffen RP, Kaplan HR. Subclasses of cyclic AMP-specific phosphodiesterase in left ventricular muscle and their involvement in regulating myocardial contractility. *Circ Res*. 1987;61:539–547.
33. Dodge KL, Khouangsathiene S, Kapiloff MS, Mouton R, Hill EV, Houslay MD, Langeberg LK, Scott JD. mAKAP assembles a protein kinase A/PDE4 phosphodiesterase cAMP signaling module. *EMBO J*. 2001;20:1921–1930.

Circulation Research
JOURNAL OF THE AMERICAN HEART ASSOCIATION

Spatiotemporal Dynamics of β-Adrenergic cAMP Signals and L-Type Ca^{2+} Channel Regulation in Adult Rat Ventricular Myocytes: Role of Phosphodiesterases

Jérôme Leroy, Aniella Abi-Gerges, Viacheslav O. Nikolaev, Wito Richter, Patrick Lechêne, Jean-Luc Mazet, Marco Conti, Rodolphe Fischmeister and Grégoire Vandecasteele

Circ Res. 2008;102:1091-1100; originally published online March 27, 2008;
doi: 10.1161/CIRCRESAHA.107.167817
Circulation Research is published by the American Heart Association, 7272 Greenville Avenue, Dallas, TX 75231

Print ISSN: 0009-7330. Online ISSN: 1524-4571

ONLINE DATA SUPPLEMENT

Spatiotemporal dynamics of β-adrenergic cAMP signals and L-type Ca^{2+} channel regulation in adult rat ventricular myocytes: Role of phosphodiesterases

Jérôme Leroy,[1,2] Aniella Abi-Gerges,[1,2] Viacheslav O. Nikolaev,[3] Wito Richter,[4] Patrick Lechêne,[1,2] Jean-Luc Mazet,[1,2] Marco Conti,[4] Rodolphe Fischmeister,[1,2] Grégoire Vandecasteele[1,2]

[1]INSERM U769, Châtenay-Malabry, France

[2]Univ Paris-Sud, Faculté de Pharmacie, Châtenay-Malabry, France

[3]Rudolf-Virchow-Center, DFG-Research Center for Experimental Biomedicine, University of Würzburg, Würzburg, Germany

[4]Division of Reproductive Biology, Department of Obstetrics and Gynecology, Stanford University School of Medicine, Palo-Alto, USA

Running title: cAMP and $I_{Ca,L}$ dynamics in cardiac myocytes

Correspondence to:
Dr. Rodolphe FISCHMEISTER
INSERM U-769
Université Paris-Sud 11
Faculté de Pharmacie
5, Rue J.-B. Clément
F-92296 Châtenay-Malabry Cedex
France

Tel. 33-1-46 83 57 71
Fax 33-1-46 83 54 75
E-mail: fisch@vjf.inserm.fr

Materials and Methods

Cardiomyocyte isolation, culture and infection

Male Wistar rats (250–300 g) were subjected to anesthesia by intraperitoneal injection of pentothal (0.1 mg/g), and hearts were excised rapidly. Individual ventricular myocytes were obtained by retrograde perfusion of the heart as previously described.[1] Freshly isolated cells were suspended in minimal essential medium (MEM: M 4780; Sigma, St Louis, MO USA) containing 1.2 mmol/L Ca^{2+}, 2.5% fetal bovine serum (FBS, Invitrogen, Cergy-Pontoise, France), 1% penicillin-streptomycin and 2% HEPES (pH 7.6) and plated on 35 mm, laminin-coated culture dishes (10 µg/mL laminin, 2 h) at a density of 10^4 cells per dish. After 1h the medium was replaced by 300 µL of FBS-free MEM. $I_{Ca,L}$ measurements were performed on non-infected myocytes, CNG channel current (I_{CNG}) measurements were performed on myocytes infected with an adenovirus encoding E583M/C460W CNGA2 (MOI=3000 pfu/cell), and FRET measurements were performed on myocytes infected with an adenovirus encoding Epac2-camps (MOI=1000 pfu/cell). In some FRET experiments, PKA was blocked by co-infecting the cells with an adenovirus encoding for rabbit muscle cAMP-dependent protein kinase inhibitor (PKI, MOI=300).[2] All experiments were performed at room temperature 24h to 48h after cell plating.

Electrophysiological Experiments

The whole cell configuration of the patch-clamp technique was used to record $I_{Ca,L}$ and I_{CNG}. Patch electrodes resistance between 0.5–1 MΩ when filled with internal solution containing (in mmol/L): CsCl 118, EGTA 5, $MgCl_2$ 4, sodium phosphocreatine 5, Na_2ATP 3.1, Na_2GTP 0.42, $CaCl_2$ 0.062 (pCa 8.5), HEPES 10, adjusted to pH 7.3. Control zero Ca^{2+}/Mg^{2+} extracellular Cs^+-Ringer solution contained (in mmol/L): NaCl 107.1, CsCl 20, $NaHCO_3$ 4, NaH_2PO_4 0.8, D-glucose 5, sodium pyruvate 5, HEPES 10, adjusted to pH 7.4. For I_{CNG}

recordings, this solution was supplemented with nifedipine (1 μmol/L) to block $I_{Ca,L}$.[1] For $I_{Ca,L}$ recordings, 1.8 mmol/L $CaCl_2$ and 1.8 mmol/L $MgCl_2$ were added to the external solution. For $I_{Ca,L}$ measurement, the cells were depolarized every 8 s from –50 to 0 mV during 400 ms. The use of –50 mV as holding potential allowed the inactivation of voltage-dependent sodium currents. Potassium currents were blocked by replacing all K^+ ions with external and internal Cs^+. For I_{CNG} measurement, the cells were maintained at 0 mV holding potential and routinely hyperpolarized every 8 s to –50 mV test potential during 400 ms. Voltage-clamp protocols were generated by a challenger/09-VM programmable function generator (Kinetic Software, Atlanta, GA, USA). The cells were voltage-clamped using a patch-clamp amplifier (model RK-400; Bio-Logic, Claix, France). Currents were analogue-filtered at 3 KHz and digitally sampled at 10 KHz using a 12-bit analogue-to-digital converter (DT2827; Data translation, Marlboro, MA, USA) connected to a compatible PC (386/33 Systempro; Compaq Computer Corp., Houston, TX, USA).

Live cell imaging

Cells were maintained in a K^+-Ringer solution containing (in mmol/L): NaCl 121.6, KCl 5.4, $MgCl_2$ 1.8; $CaCl_2$ 1.8; $NaHCO_3$ 4, NaH_2PO_4 0.8, D-glucose 5, sodium pyruvate 5, HEPES 10, adjusted to pH 7.4. Images were captured every 5 s using the 40x oil immersion objective of a Nikon TE 300 inverted microscope connected to a software-controlled (Metafluor, Molecular Devices, Sunnyvale, CA, USA) cooled charge coupled (CCD) camera (Sensicam PE; PCO, Kelheim, Germany). CFP was excited during 150-300 ms by a Xenon lamp (100 W, Nikon, Champigny-sur-Marne, France) using a 440/20BP filter and a 455LP dichroic mirror. Dual emission imaging of CFP and YFP was performed using an Optosplit II emission splitter (Cairn Research, Faversham, UK) equipped with a 495LP dichroic mirror and BP filters 470/30 and 535/30, respectively.

PDE Assay

Ventricular myocytes (2.10^5 cells) from different hearts were cultivated in laminin-coated dishes (50 mm) as described above. After 24h, the culture media was replaced by a Ringer-K^+ solution and the cells were challenged for 15 s with a given Iso concentration. After 10 min, the dishes were dipped in liquid Nitrogen and placed at -80°C. Cells were homogenized in ice-cold buffer containing (in mmol/L) NaCl 150, Tris HCL (pH 7.5) 50, Glycerol 5%, EDTA 1, EGTA 0.2, β-mercaptoethanol 5, sodium pyrophosphate 10, NaVO3 1, sodium fluoride 10, AEBSF 1, NP40 0.5%, supplemented with protease inhibitor cocktail (Roche, Basel, Switzerland) and centrifuged at 10,000 g for 10 min at 4°C. PDE activity was measured in the supernatant according to a modification of the two-step assay procedure method described by Thompson & Appleman[3] in a total volume of 500 µL including (in mmol/L) Tris-HCl 40, pH 8.0, $MgCl_2$ 10, β-mercaptoethanol 1.25 supplemented with 1 µmol/L cAMP and 10^5 cpm [^{3}H]-cAMP, as detailed previously.[4] PDE family-specific activities were determined as the difference between PDE activity in the absence of inhibitor and the residual hydrolytic activity observed in the presence of the selective inhibitor. Protein concentration was determined by Bradford assay.

Data Analysis

The maximal amplitude of $I_{Ca,L}$ was measured as the difference between the peak inward current and the current at the end of the 400 ms duration pulse. I_{CNG} amplitude is time-independent and was measured at the end of the 400 ms pulse. Currents were not compensated for capacitance and leak currents. In a total of 138 ARVMs, mean capacitance was 152.3±3.2 pF. I_{CNG} density (dI_{CNG}) was calculated for each experiment as the ratio of current amplitude to cell capacitance. In imaging experiments, average fluorescence intensity

was measured in a region of interest comprising the entire cell or a significant part of the cell. Background was subtracted and YFP intensity was corrected for CFP spillover into the 535 nm channel before calculating the CFP/YFP ratio. Ratio images were obtained with ImageJ software (National Institutes of Health). Data are represented as mean ± SEM. Kinetic parameters (t_{max} and τ_{decay}) were determined using Microsoft Excel and Origin 6 softwares. τ_{decay} values were determined by fitting the decrease phase of signals with the following single exponential equation: $y=A*\exp(-t/\tau_{decay})+B$. Statistics were performed using Origin 6 software. Statistical significance was evaluated using Student's unpaired *t* test and a difference was considered statistically significant when p was <0.05.

Drugs

Isoprenaline (Iso), acetylcholine (ACh) and 3-isobutyl-1-methylxantine (IBMX) were from Sigma (Saint Louis, MO USA). Cilostamide was from Tocris Bioscience (Ellisville, MI USA) and Ro 20-1724 was kindly provided by Hoffman-La-Roche (Basel, Switzerland).

Discussion

Although I_{CNG} and Epac2-camps have a similar sensitivity to cAMP (K_D~1 µmol/L),[2,3] the binding and dissociation kinetics of cAMP may be different. A question therefore arises whether the measured differences between the t_{max} and τ_{decay} values obtained with the two probes (Fig. 2) may result from differences in the on- (k_{on}) and off-rate (k_{off}) for cAMP binding to the probes. However, a thorough analysis of the literature indicates that this is very unlikely. *In vitro* experiments using Epac2-camps showed that the sensor responded to a 20 µmol/L jump increase in cAMP with a τ_{on} of 2 s.[4] Moreover, when 10 µmol/L bovine heart PDE was added to the cuvette, leading to a massive hydrolysis of cAMP and hence a

sudden decrease in cAMP concentration, the FRET ratio returned to basal values with a τ_{decay} of 2.9±0.3 s.[4] These τ_{on} and τ_{decay} values are much faster than on- and off-rates measured here (Fig. 2). For the double-mutant CNG channel, we found no published experimental values for either τ_{on} or τ_{decay}. However, a previous report in HEK cells transfected with the WT-CNG channel, which has an apparent K_D for cAMP of 36 μmol/L and a Hill coefficient of 2.3,[2] showed a response of I_{CNG} to a jump increase in intracellular cAMP with a τ_{on} of 212 ms.[5] In these experiments, cAMP was released by a flash photolysis of 200 μmol/L 1-(2-nitrophenyl)ethyl-cAMP, a caged cAMP analogue. Although the concentration of cAMP released by the flash was not provided in that study, we estimated it to ~28 μmol/L based on the amplitude of the response and the dose-response curve. Assuming that cAMP binds the CNG channel following first order kinetics, τ_{on} and τ_{decay} should be, respectively, $\sim 1/k_{on}/[cAMP]$ and $\sim 1/k_{off}$, with $K_D=k_{off}/k_{on}$. This allows to derive numerical values for $k_{on}=1/\tau_{on}/[cAMP]=1.7\text{x}10^5\ M^{-1}s^{-1}$, $k_{off}=K_D.k_{on}=6.1\ s^{-1}$, and $\tau_{decay}=1/k_{off}=0.16$ s. This τ_{decay} value is more than two orders of magnitude faster that the τ_{decay} measured in our experiments (33.9±2.6 s in Fig. 2E). However, the CNG channel used here had a double mutation in the cAMP binding site, which increased its affinity for cAMP ~40-fold ($K_D=0.89$ μmol/L^2). If we assume that this increased affinity is entirely due to a reduced off-rate of cAMP from the channel, τ_{decay} should increase 40-fold, i.e. to 6.4 s. This is still 5 times faster than the values obtained experimentally.

Therefore, we conclude that the on and off rates of the Iso response measured by the CNG channel and the Epac2-camps sensor in ARVMs reflect spatiotemporal changes in intracellular cAMP concentration and not differences in the characteristics of the probes.

Supplemental References

1. Rochais F, Vandecasteele G, Lefebvre F, Lugnier C, Lum H, Mazet J-L, Cooper DMF, Fischmeister R. Negative feedback exerted by PKA and cAMP phosphodiesterase on subsarcolemmal cAMP signals in intact cardiac myocytes. An *in vivo* study using adenovirus-mediated expression of CNG channels. *J Biol Chem.* 2004;279:52095-52105.

2. Rich TC, Tse TE, Rohan JG, Schaack J, Karpen JW. In vivo assessment of local phosphodiesterase activity using tailored cyclic nucleotide-gated channels as cAMP sensors. *J Gen Physiol.* 2001;118:63-77.

3. Nikolaev VO, Bunemann M, Hein L, Hannawacker A, Lohse MJ . Novel single chain cAMP sensors for receptor-induced signal propagation. *J Biol Chem.* 2004;279:37215-37218.

4. Nikolaev VO, Gambaryan S, Engelhardt S, Walter U, Lohse MJ. Real-time monitoring of live cell's PDE2 activity: Hormone-stimulated cAMP hydrolysis is faster than hormone-stimulated cAMP synthesis. *J Biol Chem.* 2005;280:1716-1719.

5. Rich TC, Fagan KA, Nakata H, Schaack J, Cooper DMF, Karpen JW. Cyclic nucleotide-gated channels colocalize with adenylyl cyclase in regions of restricted cAMP diffusion. *J Gen Physiol.* 2000;116:147-161.

Supplementary Figure Legend

Online Figure I. Effect of PDE3 and PDE4 inhibition on basal cAMP and $I_{Ca,L}$ in ARVMs. ARVMs were superfused with control Ringer solution before application of the specific PDE3 inhibitor cilostamide (Cil, 1 μmol/L), the specific PDE4 inhibitor Ro-201724 (10 μmol/L), or a combination of both. A, Time course of CFP/YFP ratio obtained from a cardiomyocyte infected with the Epac2-camps sensor is presented. Individual ratio images shown on top of the graph were acquired at the times indicated by the corresponding letters in the graph. B, Mean ± SEM of several individual experiments as in A. Selective inhibition of PDE3 (n=26) or PDE4 (n=18) resulted in a slight increase in cAMP whereas combination of both resulted in a robust cAMP elevation (n=9). C, Typical time course of $I_{Ca,L}$ recorded from a cell when Cil (1 μmol/L), Ro-201724 (10 μmol/L) or both PDEs inhibitors were applied. Individual current traces were recorded at the times indicated by the corresponding letters on the graph. D, Mean ± SEM results of 7 similar experiments as in C. $I_{Ca,L}$ potentiation was only obtained when both inhibitors were applied in combination. *, $p<0.05$ and ***, $p<0.001$ using paired *t*-test.

Supplementary Movie Description

Variation of the corrected CFP/YFP ratio coded by pseudocolors in an adult rat ventricular myocyte expressing the Epac2-camps sensor when challenged with a 15 s pulse of Isoprenaline (100 nmol/L). Pseudocolor scale as in Fig. 1.

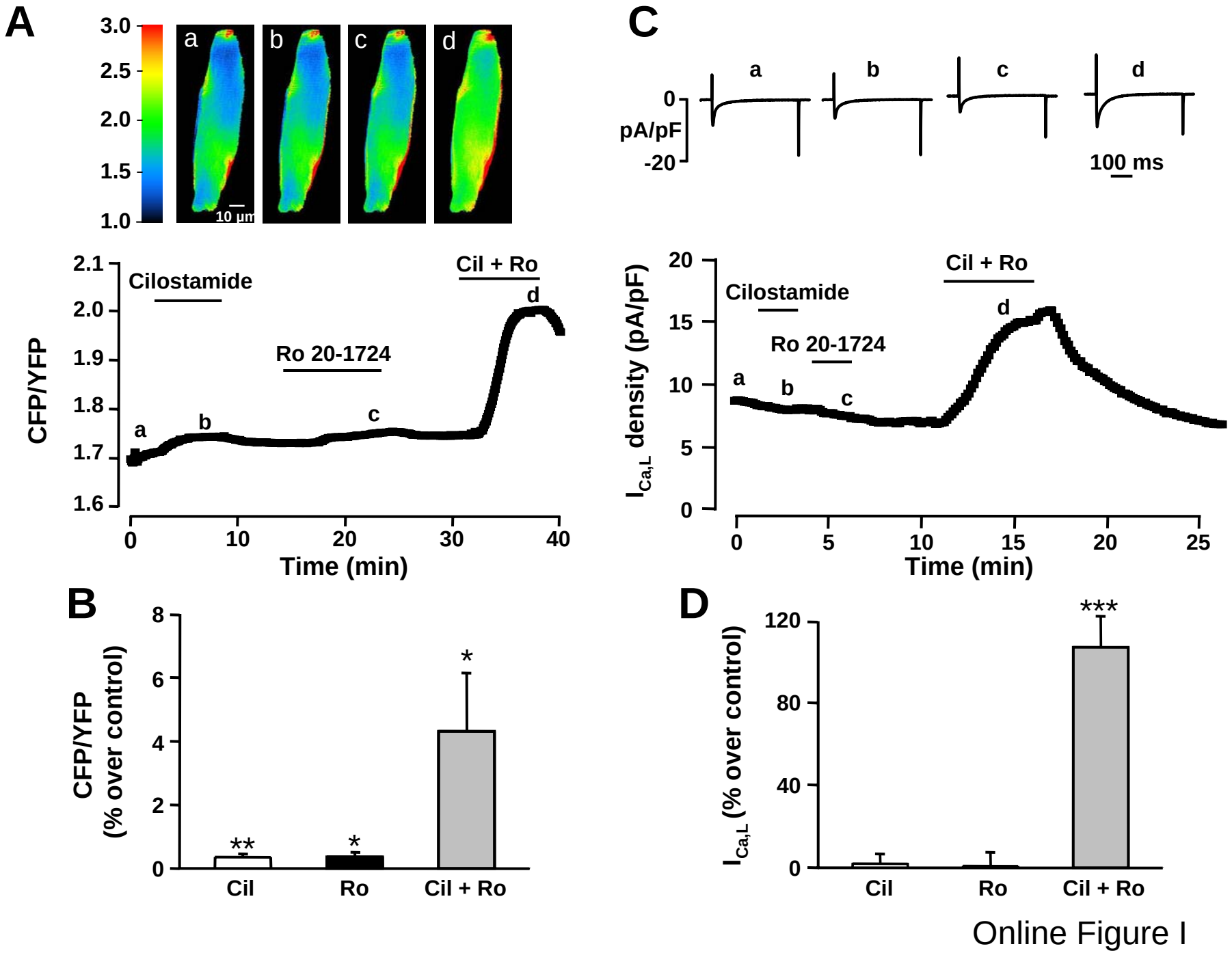

Online Figure I